URSI-RCRS 2024, ARIES/GEHU, Bhimtal, India, 22 - 25 October, 2024

Design Considerations for the Optimization of Propagation Loss of $Ge_{1-x}Si_x$-on-Al_2O_3 Optical Waveguides for the 2-µm Communication Band

Harshvardhan Kumar[1]

[1]The LNM Institute of Information Technology, Electronics and Communication Engineering Rupa ki Nangal, Post-Sumel, Via, Jamdoli JAIPUR, RAJASTHAN, IN 302031

Abstract

In this work, we present, to the best of our knowledge, the first demonstration of a low-loss $Ge_{1-x}Si_x$ -on-Al_2O_3 optical rib waveguide (WG) for the future optical communication band, which is a critical enabler of photonic integrated circuits (PICs). To achieve effective transmission in the mid-infrared (MIR) range (2-14 µm), $Ge_{1-x}Si_x$ alloys were used as the core material. The proposed rib optical WG was designed and optimized in order to achieve minimal propagation loss and a much higher power confinement factor (PCF) of the guided modes. This resulted in a PCF of up to 98% and a very low propagation loss of 8.5×10^{-3} dB/cm at 2-µm, which is the lowest known WG propagation loss, as far as we are aware. These findings show that our developed $Ge_{1-x}Si_x$ WG is feasible for future optical networking and communication.

1. Introduction

Fiber-optic networks have become extensively utilized on a global scale to facilitate high-speed communications. This can be attributed to the notable advantages they offer, including their low loss rate of ~0.2 dB/km and the wide array of optical instruments that are readily accessible for their implementation. The current utilization of 1.31 and 1.55 µm wavelengths technology has become limited as a result of the rapid growth in internet traffic[1]. To address this issue, there is a suggestion to explore alternative telecommunication bands that can offer increased capacity. In recent research, the utilization of low attenuated hollow-core photonic bandgap fiber (HC-PBGF) with minimal attenuation of approximately 0.1 dB/Km has shown promise in the development of a new spectral band for telecommunications[2]. This fiber type also offers high-speed transmission capabilities, reaching speeds of approximately 98% of the velocity of light in free space. These characteristics make HC-PBGF a potential candidate for exploring a spectral band around 2 µm in the field of telecommunications. To successfully integrate the new band, it is necessary to employ various components such as optical WGs, modulators, light sources, detectors, multiplexers and demultiplexers, as well as couplers. The integration of various functional elements into a single photonic integrated circuit (PIC) has the potential to offer a compact, cost-effective, and scalable platform. In this particular context, the development of high-bandwidth (BW) thulium-doped fiber amplifier (TDFA) light sources within the wavelength range of 1.8-2.1 µm has been explored by researchers[3]. Furthermore, a limited number of detectors based on III-V and group-IV alloys have been reported for the 2-µm band[4], [5], indicating the potential of this wavelength range as an alternative supplementary window for future high-speed optical communication systems.

To accommodate the new wavelength band of communications, it is imperative to utilize a waveguide (WG) that exhibits minimal loss and high power confinement factor (PCF). Hence, the circuit must possess the capability to efficiently guide light with minimal loss while also being compact, thereby facilitating the integration of light sources and detectors. In recent years, there has been increasing attention on the integration of group-IV photodetectors (PDs) on a silicon (Si)-based WG platform. However, it has been observed that these WGs exhibit high levels of optical loss[6]. The reduction of optical loss and the increase in the power confinement factor (PCF) are highly desirable. In recent years, researchers have successfully demonstrated several optical WGs for the 2-µm bands. These WGs were developed using different materials, including TiO2[7], SiGe[8], Si[9], Si3N4[10], and SRN[10]. Nevertheless, it is important to note that the propagation losses associated with the majority of devices continue to remain significantly high. The comparative analysis results suggest that both Si3N4 and $Ge_{1-x}Si_x$ alloy demonstrate favorable characteristics in terms of achieving low propagation loss. As well, it has been observed that the propagation loss of SiGe WG can be effectively minimized through the utilization of WG engineering techniques and the optimization of the device structure. To date, there has been a lack of research conducted on $Ge_{1-x}Si_x$ alloy-based WGs, which has impeded the progress in developing low-loss WGs for the 2-µm band.

In this work, we provide the first evidence of low propagation loss $Ge_{1-x}Si_x$-on-Al_2O_3 rib photonic WG for the emerging fiber-optic communication band (at λ = 2-µm).

2. Device, Design, and Fabrication

Fig. 1(a-b) shows the proposed WG's three-dimensional (3-D) structure and the index profile that corresponds to the cross-sectional view. Using low-energy plasma-enhanced chemical vapor deposition (LEPECVD), $Ge_{1-x}Si_x$ can be grown at a rate of 5–10 nm/s on an Al_2O_3-SiO_2 platform[11]. Optical lithography can be employed to pattern the structures, which are subsequently etched using inductively coupled plasma[12]. It is advised to have the refractive index of the core layer (n_{core}) greater than the cladding index (ncladding) and the effective index (n_{eff}) based on the physics design criteria [29]. The material used for the core layer is the $Ge_{1-x}Si_x$ alloy to comply with the above requirements. The refractive index values for $Ge_{1-x}Si_x$ alloy, SiO_2, and Al_2O_3 can be obtained from the relevant source[13], [14]. To extend the transmission window up to 5.5 µm, sapphire, also called aluminum oxide (Al_2O_3), is used in the formation of the bottom cladding layer. At wavelengths of 2 µm, the WG cross-section enables the WG to operate on its fundamental TE mode. A simulation of the intended WG structure was performed using COMSOL Multiphysics. To support the long WG, we took into consideration electromagnetic wave beam envelopes (EWBE), and we used boundary mode analysis to determine the attenuation constant and effective refractive index. Fig. 1(c-d) displays the simulation steps, the physics setup, and the propagation loss at various concentrations of Si, respectively. Increased silicon (Si) concentration in germanium (Ge) causes an increase in propagation loss, as seen in Fig. (d), which is considered undesirable. Two possible causes for the observed behavior are (i) the $Ge_{1-x}Si_x$ alloy's decreasing refractive index[13] and (ii) the impact of the effective refractive index. As a consequence, the propagation loss increases due to an increase in the imaginary effective index. The reduction in the effective refractive index will also result in a decrease in PCF. As a result, the optimal value to calculate the metrics of the proposed WG in this study has been determined to be Si = 10%.

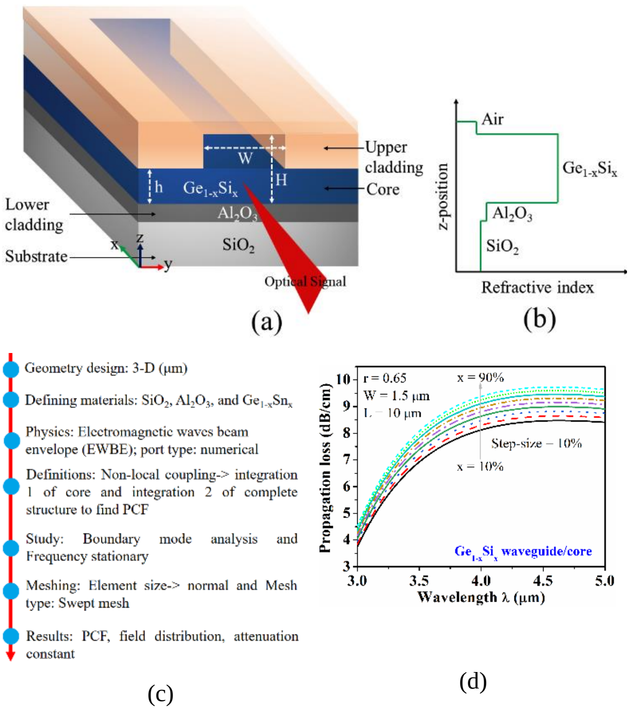

Fig. 1. (a) Three-dimensional (3-D) structural schematic of our proposed $Ge_{1-x}Si_x$-on-Al_2O_3 rib optical WG on SiO_2 substrate for sensing and emerging fiber-optic telecommunication applications. (b) Refractive index profile for the material used in the proposed WG. (c) COMSOL Multiphysics simulation steps of the proposed WG structure. (d) Calculated propagation of the proposed WG as a function of wavelength with varying Si concentration (x) for a fixed ratio of 0.65, width of 1.5 µm, and length of 10-µm.

Theoretically, the fundamental mode may be supported by the device structure by choosing the optimal rib structure aspect ratio, which can be found using the relation[15];

$$W/H \leq \alpha + \left(r/\sqrt{1-r^2}\right); \text{for } 0.5 \leq r \leq 1.0 \quad (1)$$

where, W/H is the aspect ratio of rib WG width to the height, r is the slab height to the total height of the rib WG (i.e. $r = h/H$). The value of $\alpha = 0.3$ and $H = 2\ \mu m$ was considered in this work. Next, as shown in Figure 2, the fundamental TE mode profile was simulated using the COMSOL Multiphysics software. $Ge_{0.90}Si_{0.10}$, Al_2O_3, and SiO_2 have refractive indices of 4.08, 1.6152, and 1.4379 at λ = 2 µm, respectively. The high contrast between the optical indices of $Ge_{0.90}Si_{0.10}$ and Al_2O_3 permits excellent confinement of light within the WGs (see Figs. 2a, b, and c) for a fixed width of 2 µm. However, as the ratio between the height of the slab and the total height of the rib WG (r) increases, confinement is weakened. A further observation is that the WGs are single-mode at 2 µm and can only propagate the fundamental quasi-TE mode. The proposed WG will therefore result in low propagation loss. The higher-order modes are primarily responsible for undesirable high propagation loss[16].

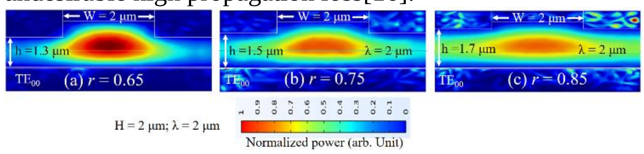

Fig. 2. The simulated fundamental quasi-TE mode profiles at λ = 2 µm for (a) r = 0.65, (b) r = 0.75, and (c) r = 0.85 with a fixed width and rib height of 2 µm.

3. Results and Discussion

The power confinement factor (PCF) is commonly defined as the ratio of the mode power flux confined within the WG region to the total power flux in an infinite region. In order to calculate the PCF, it is necessary to determine the region of the WG's cross-section. In this study, the $Ge_{0.90}Si_{0.10}$ rib WG region is chosen as the focus of the investigation. The PCF can be computed to determine the light/optical power confined within the WG core and mathematically it can be estimated as[17], [18], [19];

$$\mathrm{PCF} = \frac{\int_{-\infty}^{R} P(s).ds}{\int_{-\infty}^{\infty} P(s).ds} \quad (2)$$

In the above eqn. (2), we denote the power in the region as $P(s)$ and the WG region as R. According to the studies, it has been concluded that in order to achieve effective mode propagation in a rib WG region, the calculation method indicates that the PCF must have a minimum value of 5% or higher[20]. Fig. 3 displays the calculated PCF as a function of the rib WG width for different ratios of the height of the slab to the total height of the rib WG. In this study, the estimation of the range of rib WG width is done using Eqn. (1).

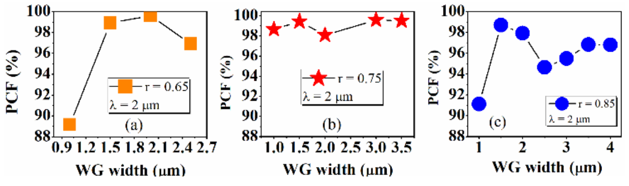

Fig. 3. Calculated power confinement factor of the designed WG at λ = 2 μm as a function of rib WG width for (a) r = 0.65, (b) r = 0.75, and (c) r = 0.85 with a fixed width and rib height of 2 μm.

The obtained results indicate that the variation in width has a substantial effect on the PCF of WG for r (ratio) values of 0.65 and 0.85. However, the impact is comparatively less prominent for r = 0.75. The observed behavior can be elucidated by considering the relationship between the effective refractive index (n_{eff}) and the width[17]. The analysis conducted indicates that the WG demonstrates a high value of PCF exceeding 98% for a specific value of r = 0.75. Thus, in order to achieve optimal performance in the communication band, it has been determined that selecting a value of r = 0.75 can be considered an optimal choice.

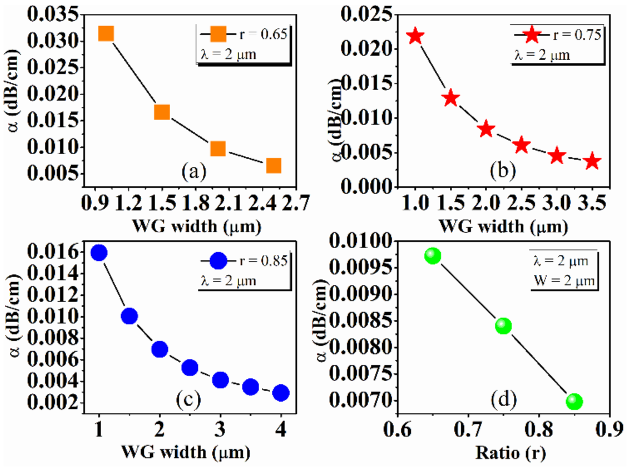

Fig. 4. Calculated propagation loss of the rib WG at λ = 2 μm for (a) r = 0.65, (b) r = 0.75, and (c) r = 0.85 for a fixed rib height of 2 μm. Fig. (d) represents the calculated loss as a function of the ratio for a fixed rib WG width and height of 2 μm at λ = 2 μm.

The propagation loss of the WG is primarily a function of the effective refractive index, specifically the imaginary effective refractive index ($Img\left[n_{eff}\right]$) and wavelength (λ). Here, the wavelength is in μm. The smaller the value of the imaginary refractive index, and consequently the lower the propagation loss. In order to propagate the utmost optical power through the WG, it is desirable to use WGs with minimal loss. Experimentally, it can be determined based on the slope of the linear variation of transmittance with WG length[11]. Theoretically, however, propagation loss (α) of the WG in various modes can be calculated by[21];

$$\alpha\ (in\ dB) = \frac{4\pi \times Img\left[n_{eff}\right]}{\lambda} 10 log_{10}(e) \cong 54.57\left(\frac{Img\left[n_{eff}\right]}{\lambda}\right) \quad (3)$$

The propagation loss in dB/cm can be calculated by taking the slope of propagation loss versus the WG's width[22]. In this work, the value of the effective refractive index was obtained using COMSOL Multiphysics software, and the mathematical expression is given as;

$$n_{eff} = \beta_1/\beta_0 = \beta_1 \lambda_0/2\pi \quad (4)$$

where, β_1 and λ_0 denote the propagation constant and operating wavelength (also known as free-space wavelength). Fig. 4 depicts the deduced propagation loss for the fundamental TE mode for r = 0.65, 0.75, and 0.85 to allow for non-destructive transmission, yielding comparable performance at λ = 2 μm. The propagation loss decreases as the ratio (r) value increases. For the optimal value of r, which is 0.75, a propagation loss of 0.0085 dB/cm is obtained with W = 2 μm, which is the lowest value compared to previously reported results at λ = 2 μm[7], [8], [9], [10]. At λ = 2 μm, this exceptionally low propagation loss value paves the way for the development of high-performance WGs for emergent fiber-optic communication.

Next, the effect of Al_2O_3 (lower cladding) layer thickness ($t_{Al_2O_3}$) on the effective refractive index, PCF, and propagation loss of a rib WG is investigated. This study aims to achieve the optical thickness of the Al_2O_3 layer in order to obtain the highest power confinement factor and lowest propagation loss. As shown in Figure 5 (a), the effective refractive index is independent of the thickness of Al_2O_3. However, the imaginary component of the effective refractive index is highly dependent on the thickness of Al_2O_3. As shown in Figure 5(a), as the Al_2O_3 thickness increases, the imaginary part increases considerably, and the propagation loss exhibits the same behavior (see Fig. 5(b)). The PCF is less affected by variations in Al_2O_3 thickness, and its value is nearly constant in the thickness range of 50 to 60 nm. The result also implies that reduced propagation may be achieved by depositing a thin layer of Al_2O_3. Growing an Al_2O_3 layer less than 50 nm is challenging. Therefore, the 50 nm thickness of Al_2O_3 has been selected as the optimal thickness from the fabrication standpoint in order to assess the performance of the proposed WG.

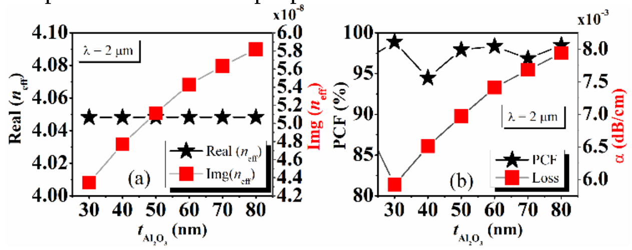

Fig. 5. (a) Calculated effective refractive index as a function of Al_2O_3 layer thickness. (b) Calculated PCF and propagation loss as a function of Al_2O_3 layer thickness at λ = 2 μm.

The benchmarking results for propagation loss in various materials used for the design and fabrication of optical waveguides operating at a wavelength of 2 μm are presented in Table 1. The results of the comparative analysis indicate that both Si_3N_4 and $Ge_{1-x}Si_x$ alloy exhibit promising characteristics for achieving low propagation loss. In previous studies, various WGs have been investigated. However, our research focuses on a novel $Ge_{0.90}Si_{0.10}$-on-Al_2O_3 rib waveguide. Our findings indicate that this particular waveguide demonstrates the lowest propagation loss when the waveguide structure is optimized. The proposed WG operating at the 2 μm band holds significant potential for various applications such as on-chip optical interconnect, sensing, spectroscopy, and emerging fiber-optic telecommunication applications.

Table 1. Comparative analysis of propagation loss of different optical waveguides to date used for data transmission at 2 μm

Materials	*n*	α (dB/cm)	Year	Method*	Ref.
TiO_2	2.31	6	2017	Num. Sim. and Exp.	[7]
$Si_{0.8}Ge_{0.2}$	3.54	2	2017	Exp.	[8]
Si	3.45	<3	2019	Exp.	[9]
Si_3N_4	2.0	<1	2019	CFD and Exp.	[10]
SRN	2.53	2	2019	CFD and Exp.	[10]
$Ge_{0.9}Si_{0.1}$	4.08	0.0085	---	FEM Sim.	This work

*Note: Num. Sim. → numerical simulation, Exp. → experimental, CFD → commercial finite difference Eigenmode solver, and FEM → finite element method Eigenmode solver

4. Conclusion

In conclusion, the successful demonstration of $Ge_{1-x}Si_x$-on-Al_2O_3 low-loss optical waveguides for the 2 um bands has been achieved. The proposed WG is implemented by utilizing the finite element method (FEM) Eigenmode solver. To the best of our knowledge, we achieved the lowest propagation loss (8.5×10^{-3} dB/cm) and the highest PCF (>98%). We show that both the PCF and propagation loss can be enhanced by adjusting the aspect ratio (W/H) and slab height to the total height of the rib WG (r). This study presents a comprehensive investigation of the design and analysis of high-performance GeSi-based waveguides (WG) specifically tailored for the 2-μm telecommunication band. The aim of this demonstration is to showcase a feasible method that can be employed to achieve optimal performance in $Ge_{1-x}Si_x$-based WG devices.

5. Acknowledgements

Dr. Rikmantra Basu at the National Institute of Technology Delhi, New Delhi, India, and Dr. P. Susthitha Menon at the National University of Malaysia, Malaysia, provided the authors with insightful discussions.

6. References

[1] A. D. Ellis, J. Zhao, and D. Cotter, "Approaching the Non-Linear Shannon Limit," *J. Light. Technol.*, vol. 28, no. 4, pp. 423–433, 2010, doi: 10.1109/JLT.2009.2030693.

[2] P. J. Roberts *et al.*, "Ultimate low loss of hollow-core photonic crystal fibres," *Opt. Express*, vol. 13, no. 1, pp. 236–244, 2005, doi: 10.1364/opex.13.000236.

[3] Z. Li *et al.*, "Diode-pumped wideband thulium-doped fiber amplifiers for optical communications in the 1800 – 2050 nm window," *Opt. Express*, vol. 21, no. 22, p. 26450, 2013, doi: 10.1364/oe.21.026450.

[4] Y. Chen *et al.*, "Dynamic model and bandwidth characterization of InGaAs/GaAsSb type-II quantum wells PIN photodiodes," *Opt. Express*, vol. 26, no. 26, p. 35034, 2018, doi: 10.1364/oe.26.035034.

[5] H. Kumar, Q. Chen, and C. S. Tan, "Lateral GeSn waveguide-based homojunction phototransistor for next-generation 2000 nm communication and sensing applications," *Semicond. Sci. Technol.*, vol. 38, pp. 1–10, 2023, doi: https://doi.org/10.1088/1361-6641/acb0f5.

[6] Y. H. Peng, H. H. Cheng, V. I. Mashanov, and G. E. Chang, "GeSn p-i-n waveguide photodetectors on silicon substrates," *Appl. Phys. Lett.*, vol. 105, no. 23, pp. 231109(1–4), 2014, doi: 10.1063/1.4903881.

[7] M. Lamy, C. Finot, J. Fatome, J. Arocas, J. C. Weeber, and K. Hammani, "Demonstration of high-speed optical transmission at 2 μm in titanium dioxide waveguides," *Appl. Sci.*, vol. 7, no. 6, 2017, doi: 10.3390/app7060631.

[8] M. Lamy *et al.*, "Ten gigabit per second optical transmissions at 1.98 μm in centimetre-long SiGe waveguides," *Electron. Lett.*, vol. 53, no. 17, pp. 1213–1214, 2017, doi: 10.1049/el.2017.1961.

[9] M. Lamy *et al.*, "Silicon waveguides for high-speed optical transmissions and parametric conversion around 2 μm," *IEEE Photonics Technol. Lett.*, vol. 31, no. 2, pp. 165–168, 2019, doi: 10.1109/LPT.2018.2887312.

[10]M. Lamy *et al.*, "Si and Si-rich silicon-nitride waveguides for optical transmissions and nonlinear applications around 2 μm," *Int. Conf. Transparent Opt. Networks*, vol. 2019-July, no. 19, pp. 5165–5169, 2019, doi: 10.1109/ICTON.2019.8840351.

[11]J. M. Ramirez *et al.*, "Graded SiGe waveguides with broadband low-loss propagation in the mid infrared," *Opt. Express*, vol. 26, no. 2, pp. 870–877, 2018, doi: 10.1364/oe.26.000870.

[12]Q. Liu *et al.*, "Mid-infrared sensing between 5.2 and 6.6 μm wavelengths using Ge-rich SiGe waveguides [Invited]," *Opt. Mater. Express*, vol. 8, no. 5, p. 1305, 2018, doi: 10.1364/ome.8.001305.

[13]J. Humlíček, A. Röseler, T. Zettler, M. G. Kekoua, and E. V. Khoutsishvili, "Infrared refractive index of germanium–silicon alloy crystals," *Appl. Opt.*, vol. 31, no. 1, pp. 90–94, 1992, doi: 10.1364/ao.31.000090.

[14]J. Kischkat *et al.*, "Mid-infrared optical properties of thin films of aluminum oxide, titanium dioxide, silicon dioxide, aluminum nitride, and silicon nitride," *Appl. Opt.*, vol. 51, no. 28, pp. 6789–6798, 2012, doi: 10.1364/AO.51.006789.

[15]R. A. Soref, J. Schmidtchen, and K. Petermann, "Large Single-Mode Rib Waveguides in GeSi-Si and Si-on-SiO2," *IEEE J. Quantum Electron.*, vol. 27, no. 8, pp. 1971–1974, 1991, doi: 10.1109/3.83406.

[16]H. Kumar and A. K. Pandey, "Numerical investigation of a Ge 1 − x Sn x -on-AlN waveguide and its sensing mechanism for the detection of trace gases in the mid-infrared regime," *J. Opt. Soc. Am. B*, vol. 40, no. 6, pp. 1427–1434, 2023, doi: https://doi.org/10.1364/JOSAB.484610.

[17]H. Huang, K. Liu, B. Qi, and V. J. Sorger, "Re-analysis of single-mode conditions for silicon rib waveguides at 1550 nm wavelength," *J. Light. Technol.*, vol. 34, no. 16, pp. 3811–3817, 2016, doi: 10.1109/JLT.2016.2579163.

[18]"Photon Design," FIMMWAVE version 6.1.1 manual. [Online]. Available: https://www.photond.com/

[19]J. T. Robinson, K. Preston, O. Painter, and M. Lipson, "First-principle derivation of gain in high-index-contrast waveguides," *Opt. Express*, vol. 16, no. 21, p. 16659, 2008, doi: 10.1364/oe.16.016659.

[20]D. Dai and Z. Sheng, "Numerical analysis of silicon-on-insulator ridge nanowires by using a full-vectorial finite-difference method mode solver," *J. Opt. Soc. Am. B*, vol. 24, no. 11, pp. 2853–2859, 2007, doi: 10.1364/josab.24.002853.

[21]W. Du, Z. Chen, and F. Zhao, "Analysis of single-mode optical rib waveguide in silicon carbide," *Microw. Opt. Technol. Lett.*, vol. 55, no. 11, pp. 2636–2640, 2013, doi: 10.1002/mop.27895.

[22]S. C. K. Goh *et al.*, "Monolithic Germanium-Tin Pedestal Waveguide for Mid-Infrared Applications," *IEEE Photonics J.*, vol. 13, no. 2, 2021, doi: 10.1109/JPHOT.2021.3059452.